

Jonathan E. Pleim\* and Jason K.S. Ching\*

National Oceanic and Atmospheric Administration, Air Resources Laboratory  
 Atmospheric Sciences Modeling Division, RTP, NC

303176

ABSTRACT

The Regional Acid Deposition Model (RADM) has been applied to several of the field experiments which were part of the Acid Models Operational and Diagnostic Evaluation Study (Acid MODES). The experiment which was of particular interest with regards to ozone photochemistry involved horizontal zig-zag flight patterns (ZIPPER) over an area from the eastern Ohio River valley to the Adirondacks of New York. Model simulations by both the standard resolution RADM ( $\Delta x = 80$  km) and the nested grid RADM ( $\Delta x = 26.7$  km) compare well to measurements in the low emission regions in central Pennsylvania and upstate New York, but underestimate in the high emission upper Ohio River valley. The nested simulation does considerably better, however, than the coarse grid simulation in terms of horizontal pattern and concentration magnitudes. Analysis of  $\text{NO}_x$  and  $\text{HO}_x$  concentrations and photochemical production rates of ozone show that the model's response to large point source emissions is very unsystematic both spatially and temporally. This is due to the models inability to realistically simulate the small scale (subgrid) gradients in precursor concentrations in and around large point source plumes.

performance under clear sky conditions, were flown in a corridor extending from the eastern Ohio River Valley to northeastern New York. This study focuses on the ZIPPER flights, a horizontal zig-zag pattern flown within the mixed layer (about 1300 m AGL), in order to discern horizontal spatial patterns and gradients. Both aircraft recorded continuous measurements of gaseous  $\text{SO}_2$ ,  $\text{NO}$ ,  $\text{NO}_2$ ,  $\text{NO}_y$ ,  $\text{O}_3$ ,  $\text{H}_2\text{O}_2$ , and  $\text{CO}$  as well as ambient temperature, moisture, pressure, and winds.

3 DESCRIPTION OF MODEL

The Regional Acid Deposition Model (RADM) is a comprehensive Eulerian atmospheric chemistry grid model which includes state-of-science representations of gas-phase chemistry, advective transport, subgrid vertical mixing, dry deposition and cloud processes including aqueous chemistry, convective mixing, and wet deposition (Chang et al., 1991). The modeling system incorporates hourly emission inventories, both anthropogenic and biogenic, land-use information, and gridded hourly meteorological fields provided by simulations of the Mesoscale Meteorological Model, Version 4 (MM4) with 4-D data assimilation (Stauffer et al., 1990). In addition to the standard regional scale version of RADM which has a horizontal grid cell size of 80 km, a nested grid version of RADM (Pleim et al, 1991) which increases horizontal resolution by a factor of 3 ( $\Delta x = 80 \text{ km}/3 = 26.67$  km) is used in this study in an attempt to investigate the effects of model resolution on mesoscale ozone simulation. A revision to the model since the description by Chang et al. (1991) is the addition of a non-local closure scheme for subgrid vertical transport in the convective boundary layer called the Asymmetric Convective Model (Pleim and Chang, 1992).

1. INTRODUCTION

Photochemical Eulerian grid models are being increasingly relied upon for understanding, assessment, and regulation of meso-scale and regional ozone problems. Therefore, it is extremely important to understand the realism and limitations of these models. It is often assumed that if grid resolution is made sufficiently small the model can realistically simulate the complex interactions of photochemistry and dynamic transport and dispersion processes. This is true only where the grid can sufficiently resolve the gradients of reacting chemical species. As modeling emphasis shifts from small urban areas to larger regions (e.g. Southern Oxidant Study, Lake Michigan Ozone Study, San Joaquin Air Quality Study), models with coarser grid resolution are being applied to photochemical problems. These modeling efforts are complicated by the presence of very large point source plumes which dominate  $\text{NO}_x$  emissions in many areas. Ozone formation associated with power plant plumes has been observed many times (Davis et al., 1974; Miller et al., 1978; Gillani and Wilson, 1980). Since ozone photochemistry is a notoriously non-linear process, the ability of Eulerian grid models to simulate ozone production in the vicinity of large point source plumes, where gradients of precursor concentrations are particularly severe, needs to be assessed.

4. COMPARISON OF MEASURED AND MODELED OZONE CONCENTRATIONS ON A REGIONAL SCALE

Figure 1 shows the horizontal spatial distribution of ozone measured along the ZIPPER flight path (zig-zag line in Fig 1) and interpolated between the flight legs using a simple inverse distance weighting technique. In order to facilitate comparison with model simulations, the measured and interpolated values are spatially averaged onto the same grid used by the nested grid model ( $\Delta x = 26.7$  km). Direct comparison to model simulations is complicated by the fact that the ZIPPER aircraft measurements took almost 4 hours to complete (1530 - 1920 GMT). Model simulations of this period, however, showed only small changes with time. Therefore, ozone concentrations at 18 GMT as simulated by the nested and coarse grid models are shown in Figure 2 for comparison to Figure 1. Model level 5 (~600-900 m) was used for comparison to the aircraft measurements even though the aircraft's altitude was mostly in level 6 because the current model generally underestimated the height of the convective mixed layer and level 5 is the highest model layer which was

2. DESCRIPTION OF AIRCRAFT MEASUREMENTS

The specific measurements involved in this study were made by two specially instrumented aircraft on August 31, 1988 as part of AcidMODES. Two types of flight patterns, designed to diagnose various aspects of RADM

\*On assignment to the Atmospheric Research and Exposure Assessment Laboratory, U.S. Environmental Protection Agency.

entirely within the model's mixed layer for the duration of the flight.

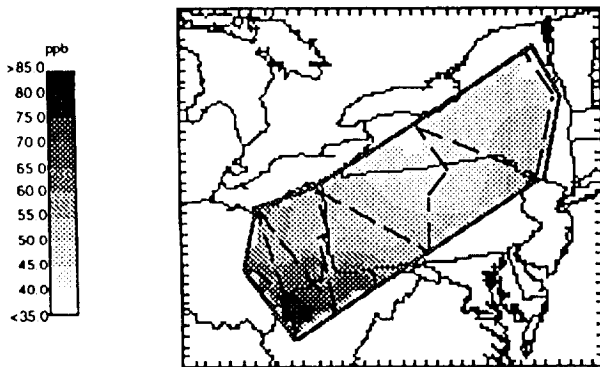


Figure 1. Airborne ozone concentration (ppb) measurements along ZIPPER flight path and interpolated between legs. Data is averaged onto a grid with 26.7 km grid cells (same as nested grid model).

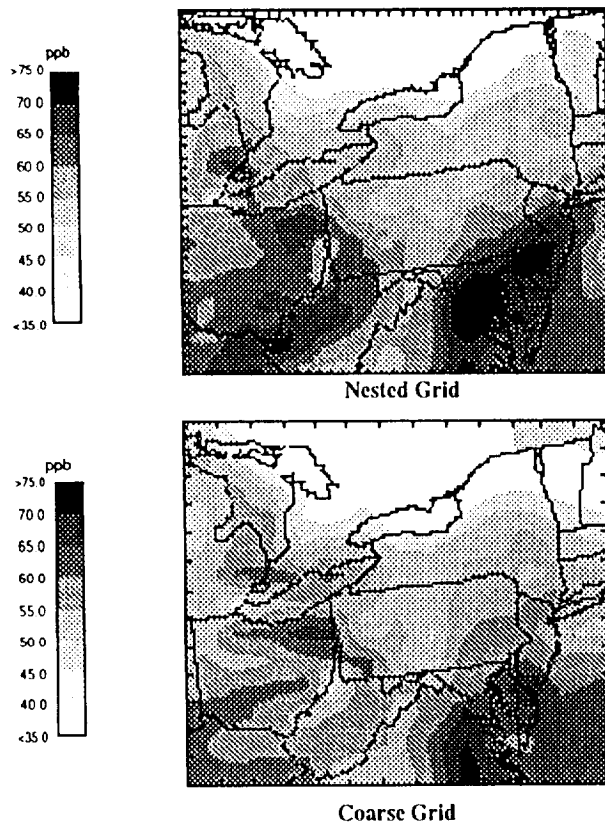


Figure 2. Ozone concentration (ppb) simulated by the nested RADM ( $\Delta x = 26.6$  km) and coarse grid RADM ( $\Delta x = 80$  km) in level 5 (~600-900m AGL) at 18 GMT.

Both nested and coarse grid model results (Figure 2) show very good similarity in terms of both spatial pattern and concentration magnitude to the measurements in the low emission regions in the northeastern portion of the ZIPPER. Throughout central and eastern PA and NY both model simulations are mostly within about 5 ppb of the measurements. In the higher  $\text{NO}_x$  emission region near the eastern Ohio River valley, however, the two simulations diverge significantly from each other and the measurements. For example, the location of the pronounced depression in the ozone concentration field near the OH-PA-WV border was simulated with much better accuracy by the nested model but the depth of the hole was

more closely simulated by the coarse grid model, although some 80-90 km to the south. The ozone maximum measured at the southmost ZIPPER corner near the Ohio river and into West Virginia (Figure 1) shows a broad area of concentrations in the 80-85 ppb range with a peak at about 85 ppb. The nested model simulation shows peak concentrations in this same area of 70-75 ppb at 18 GMT while the coarse grid simulation shows concentrations of 55-60 ppb in this area increasing to 60-65 ppb to the southwest (downwind). In general the nested model shows a marked improvement over the coarse grid simulation in the high emission Ohio River Valley region but is still unable to simulate the peak measured values.

## 5. ANALYSIS OF OZONE FORMATION IN THE OHIO VALLEY REGION

In this section the high ozone concentration region encountered by the aircraft near the southern end of the last corner in the ZIPPER flight path is further examined in an attempt to understand how the model simulates ozone formation in the vicinity of very large  $\text{NO}_x$  emitting elevated point sources. This section of the flight (~100 km long), where the aircraft crosses the Ohio River into WV and then doubles back into Ohio, is shown as a time series of 5 second average ozone and  $\text{NO}_y$  concentration data in Figure 3. The two peaks in the  $\text{NO}_y$

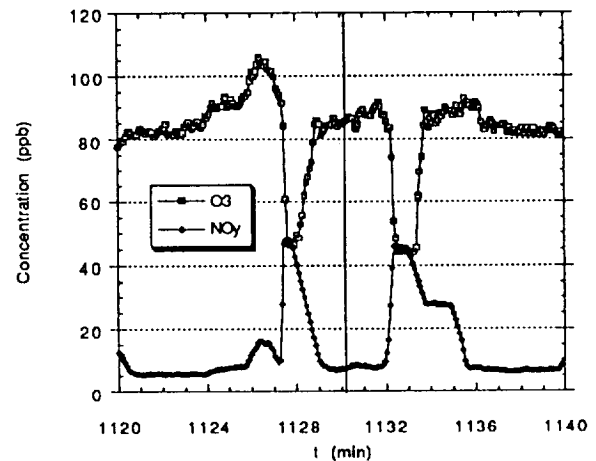


Figure 3. Time series of aircraft measurements of ozone and  $\text{NO}_y$  during ZIPPER flight when the G-1 aircraft flew through the same plume in western WV twice. The vertical line through the middle of the plot indicates where the aircraft made a 180° turn.

concentration which coincide with sharp holes in the ozone field are clear indications that the aircraft flew through freshly emitted plumes. In fact, since the aircraft turned around at the southern corner of the ZIPPER (western WV) in the middle of this time series (indicated by the vertical line in Figure 3), the two  $\text{NO}_y$  peaks are actually the same plume sampled twice. Using data from the navigational system onboard the aircraft the source of the plume was identified as a power plant which emits about 50,000 tons/year of  $\text{NO}_x$  located in southwestern West Virginia near Charleston. During the first pass the aircraft was about 3 km from the source and about 6 km on the second pass. The location of the ozone depression corresponds very closely with the  $\text{NO}_y$  peak due to the deple-

tion of ozone by reaction with freshly emitted NO in the plume. The peak in ozone concentration, up to 105 ppb on the first pass, immediately to the northwest of the ozone hole indicates photochemical production of ozone at the periphery of the plume where ambient air with VOCs and radicals is rapidly mixed with the NO<sub>x</sub> emissions. The smaller peak in the NO<sub>y</sub> profile which coincides with the ozone peak in the first pass through the plume suggests that this is a more dilute portion of the plume which broke away from the main plume and mixed more quickly with background air.

These measurements are an example of photochemical ozone production occurring very close to the source in large point source plumes. Plume photochemistry can be understood in terms of three stages (Gillani and Wilson 1980). The first stage is characterized by very concentrated NO causing a distinct depression in the background ozone field. In stage two, ozone starts to be photochemically produced at the plume edges where the NO<sub>x</sub> has been sufficiently diluted with background VOCs and radicals to not only cause ozone levels to recover their background concentrations but to exceed them. A plume is in stage three when the ozone depression in the plume center, which still exists at stage two, is no longer evident. The aircraft measurements shown in Figure 3 seem to be an example of the early phases of a stage 2 plume since the plume core still shows a significant ozone deficit while the edges, particularly the north side of the first pass, show ozone excess.

The simulation of plume photochemistry by Eulerian grid models is quite different from the three stages described above. The evolution of plume chemistry is closely coupled to plume dispersion, however, this entire process is subgrid to models which have grid cell sizes on the order of tens of kilometers. Therefore, by examining the nested model simulation in this same area we hope to learn more about the model's response to plume photochemistry. Figure 4 shows several chemical quantities as simulated by the nested grid model at 17 GMT. The first plot (top) shows NO<sub>x</sub> concentration at level 5 (~900 m). NO<sub>x</sub> is clearly dominated by urban areas and the many coal-fired power plants along the upper Ohio River. The second plot (middle) shows HO<sub>x</sub> (HO+HO<sub>2</sub>) concentrations which very closely anti-correlate with NO<sub>x</sub> concentration. This is because the radical termination reactions are proportional to NO<sub>x</sub> concentration while radical initiation reactions are not, thereby resulting in net radical depletion where NO<sub>x</sub> concentrations are high. For this discussion, the HO<sub>x</sub> field is used as a surrogate for total radicals. Similarly, the rate of reaction between NO and HO<sub>2</sub>, which is shown in the third plot (bottom), should be a good surrogate for photochemical ozone production by both HO<sub>2</sub> and RO<sub>2</sub> reactions. This plot shows peaks of ozone formation rates in regions of moderate NO<sub>x</sub> concentration such as southwestern WV and near Washington DC. Where NO<sub>x</sub> is highest, such as near the OH-PA-WV border and the western tip of Lake Erie, the radicals have been terminated to such a degree that the NO-radical reactions are relatively slow. Therefore, ozone formation is slower than ozone titration by NO emissions resulting in relative minima in the ozone field. Near the plume in southwest WV, on the other hand, NO<sub>x</sub> concentrations are considerably lower and HO<sub>x</sub> concentration much higher resulting in a favorable mix for ozone production. Note that, the greater amount of ozone formation in the Washington area (see the ozone plots in Figure 2) may be due to the greater amounts of

VOC's in the urban plumes and the more diffuse nature of the NO<sub>x</sub> emissions (mostly area rather than point sources).

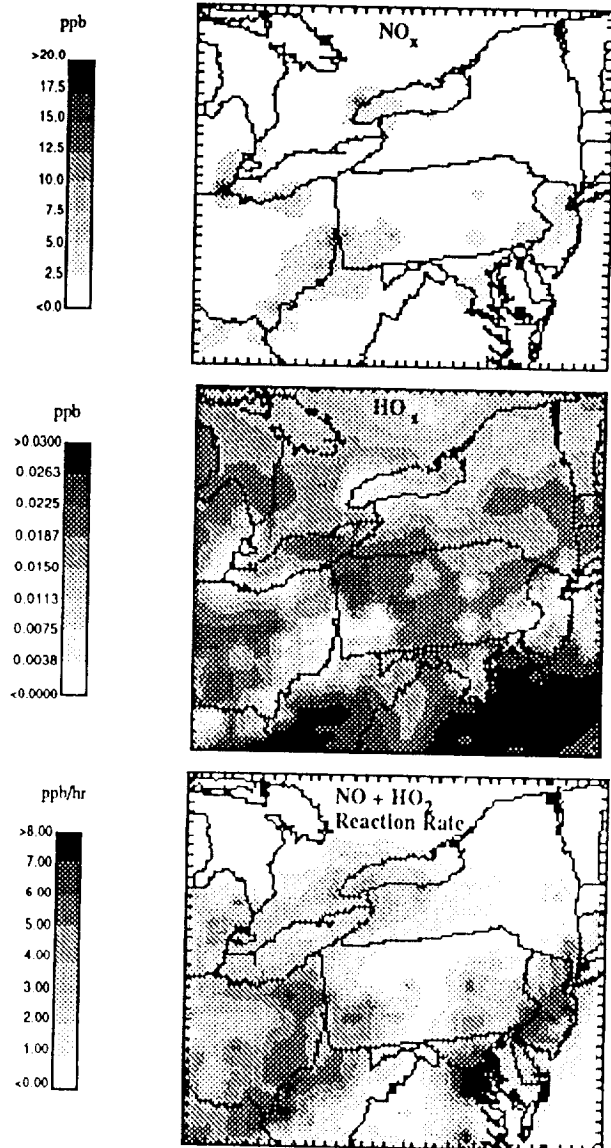


Figure 4. Nested model simulations in level 5 at 17 GMT on August 31, 1988 of NO<sub>x</sub> concentration (top), HO<sub>x</sub> concentration (middle), and rate of reaction between HO<sub>2</sub> and NO (bottom).

In order to further investigate the model's behavior, a set of time series for the grid cell in southwest WV where the nested simulation shows an isolated peak in ozone formation are shown in Figure 5. The plots are for model level 1 (~0-80 m) where hours 0-31 correspond to 00 GMT 8/31/88 - 07 GMT 9/1/88. The daytime rise in ozone concentration of about 40 ppb from hour 11 to hour 13 is coincident with a peak in the reaction rate between NO and HO<sub>2</sub> at 12 GMT of about 20 ppb/hr thereby showing the ozone increase to be primarily photochemical. The reason for this sharp peak in ozone formation can be understood through examination of NO and HO<sub>x</sub> concentrations. NO concentrations begin increasing at 11 GMT (7 am EDT), probably from the morning rush hour in nearby cities such as Charleston, WV, while HO<sub>x</sub> concentration initially rises in the morning, peaking at 12 GMT, then plunges to a minimum at 15 GMT. Therefore, the rapid

ozone formation at 12 GMT results from the combination of the onset of significant photochemistry, causing an increase in  $\text{HO}_x$  concentration, and increasing  $\text{NO}$  emissions. These favorable conditions, however, are short lived since the continuing rise in  $\text{NO}$  concentration leads to a decrease in  $\text{HO}_x$ , and by analogy other radical species. Thus, the phenomena of isolated peaks of ozone production, which was seen in the spatial model fields, is also evident in the temporal dimension such that ozone production during a single hour can dominate when conditions are most favorable.

## 6. DISCUSSION AND SUMMARY

In general, whether a particular grid cell containing a large point source plume results in an overestimation or underestimation of ozone production depends on a variety of factors such as emission rate, grid cell size, dispersion (wind speed and mixing height), and chemical background (VOCs and radicals). Thus, for the same conditions, models of different grid resolution may result in quite different simulations. The problem is the grid model's inability to simulate the subgrid processes of plume chemistry. The particular case discussed here suggests that increasing grid resolution from 80 km to 26.7 km improves the simulation of ozone formation. The highest ozone concentrations observed by the ZIPPER flights in the area downwind of the large point source plumes in the eastern Ohio Valley, however, were significantly underestimated even by the nested model. Analysis of the nested model simulation of this area shows that just a few grid cells, which happened to have a favorable mix of precursors, were responsible for the bulk of the ozone formed in this region. In addition, the time series in Figure 5 show that in these grid cells ozone formation occurred very sporadically when changing concentrations were briefly favorable for ozone formation. To improve model performance subgrid plume chemistry should be simulated either by a reactive plume/puff model or through parameterization of subgrid chemistry based on emissions, chemical and meteorological conditions.

## REFERENCES

- Chang J. S., Principal Author. (1991) The Regional Acid Deposition Model and Engineering Model. NAPAP State of Science/Technology Report 4; In: National Acid Precipitation Assessment Program: Acid Deposition State of Science and Technology, Volume I. NAPAP, Washington, DC.
- Davis D. D., Smith G. and Klauber G. (1974) Trace gas analysis of power plant plumes via aircraft measurement:  $\text{O}_3$ ,  $\text{NO}_x$ ,  $\text{SO}_2$  chemistry. *Science*, **186**, 733-736.
- Gillani N. V. and Wilson W. E. (1980) Formation and transport of ozone and aerosols in power plant plumes. *Annals N.Y. Acad. Sci.*, **338**, 276-296.
- Miller D. F., Alkezweeny A. J., Hales J. M. and Lee R. N. (1978) Ozone formation related to power plant emissions. *Science*, **202**, 1186-1188.
- Pleim, J. E., Chang J. S., and Zhang K. (1991) A nested grid mesoscale atmospheric chemistry model, *J. Geophys. Res.*, **96**, 3065-3084.
- Pleim, J. E. and Chang J. S. (1992) A non-local closure model for vertical mixing in the convective boundary layer. *Atmos. Environ.*, **26A**, 965-981.

Stauffer D. R. and Seaman N. L. (1990) Use of four-dimensional data assimilation in a limited-area model. Part I: Experiments with synoptic scale data. *Mon Wea. Rev.*, **118**, 1250-1277.

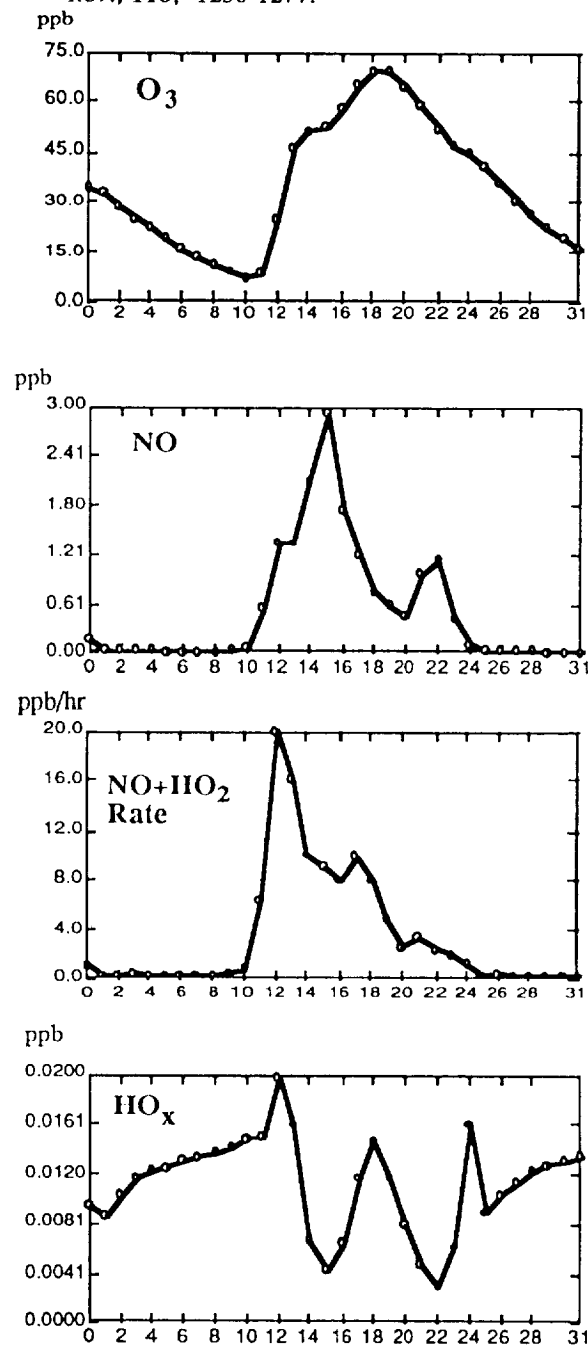


Figure 5. Time series (00 GMT 8/31/88 - 07 GMT 9/1/88) of nested model simulations in the grid cell corresponding to the plume encountered by the G-1 aircraft shown in Figure 3. From the top, the plots show  $\text{O}_3$ ,  $\text{NO}$ , rate of the reaction between  $\text{HO}_2$  and  $\text{NO}$ , and  $\text{HO}_x$  in model level 1 (~0-80 km).

## DISCLAIMER

This paper has been reviewed in accordance with the U.S. Environmental Protection Agency's peer and administrative review policies and approved for presentation and publication. Mention of trade names or commercial products does not constitute endorsements or recommendation for use.